BOSTER
antibody and ELISA experts

BOSTER BIOLOGICAL TECHNOLOGY
3942 B Valley Ave, Pleasanton, CA 94566
888-466-3604 | support@bosterbio.com | www.bosterbio.com

Anti-HMGB1 Antibody Picoband®

Catalog Number: A00066-1

About HMGB1

High mobility group box 1 protein, also known as high-mobility group protein 1 (HMG-1) and amphoterin, is a protein that in humans is encoded by the HMGB1 gene. This gene encodes a protein that belongs to the High Mobility Group-box superfamily. The encoded non-histone, nuclear DNA-binding protein regulates transcription, and is involved in organization of DNA. This protein plays a role in several cellular processes, including inflammation, cell differentiation and tumor cell migration. Multiple pseudogenes of this gene have been identified. Alternative splicing results in multiple transcript variants that encode the same protein.

Overview

Product Name	Anti-HMGB1 Antibody Picoband®
Reactive Species	Human, Mouse, Rat
Description	Boster Bio Anti-HMGB1 Antibody Picoband® catalog # A00066-1. Tested in Flow Cytometry, IF, IHC, ICC, WB applications. This antibody reacts with Human, Mouse, Rat. The brand Picoband indicates this is a premium antibody that guarantees superior quality, high affinity, and strong signals with minimal background in Western blot applications. Only our best-performing antibodies are designated as Picoband, ensuring unmatched performance.
Application	Flow Cytometry, IF, IHC, ICC, WB
Clonality	Polyclonal
Formulation	Each vial contains 4mg Trehalose, 0.9mg NaCl, 0.2mg Na2HPO4, 0.05mg NaN3.
Storage Instructions	Store at -20˚C for one year from date of receipt. After reconstitution, at 4˚C for one month. It can also be aliquotted and stored frozen at -20˚C for six months. Avoid repeated freeze-thaw cycles.
Host	Rabbit
Uniprot ID	P09429

Technical Details

Immunogen	A synthetic peptide corresponding to a sequence at the C-terminus of human HMGB1, identical to the related mouse and rat sequences.
Recommended Detection Systems	Boster recommends Enhanced Chemiluminescent Kit with anti-Rabbit IgG (EK1002) for Western blot, and HRP Conjugated anti-Rabbit IgG Super Vision Assay Kit (SV0002-1) for IHC(P) and ICC.
Cross Reactivity	No cross-reactivity with other proteins
Isotype	Rabbit IgG
Form	Lyophilized

BOSTER BIOLOGICAL TECHNOLOGY
3942 B Valley Ave, Pleasanton, CA 94566
888-466-3604 | support@bosterbio.com | www.bosterbio.com

Concentration	Adding 0.2 ml of distilled water will yield a concentration of 500 ug/ml.
Purification	Immunogen affinity purified.
Suggested Dilutions	Immunohistochemistry (Paraffin-embedded Section), 0.5-1ug/ml, Human, Mouse, Rat Western blot, 0.1-0.5ug/ml, Human, Mouse, Rat Immunocytochemistry/Immunofluorescence, 2ug/ml, Human Flow Cytometry (Fixed), 1-3ug/1x10^6 cells, Human

BOSTER BIOLOGICAL TECHNOLOGY
3942 B Valley Ave, Pleasanton, CA 94566
888-466-3604 | support@bosterbio.com | www.bosterbio.com

Anti-HMGB1 Antibody Picoband® (A00066-1) Images

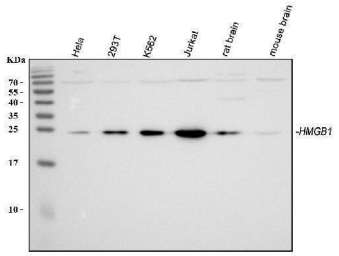

Western blot analysis of HMGB1 using anti-HMGB1 antibody (A00066-1). Electrophoresis was performed on a 5-20% SDS-PAGE gel at 70V (Stacking gel) / 90V (Resolving gel) for 2-3 hours. The sample well of each lane was loaded with 30 ug of sample under reducing conditions. Lane 1: human Hela whole cell lysates, Lane 2: human 293T whole cell lysates, Lane 3: human K562 whole cell lysates, Lane 4: human Jurkat whole cell lysates, Lane 5: rat brain tissue lysates, Lane 6: mouse brain tissue lysates. After electrophoresis, proteins were transferred to a nitrocellulose membrane at 150 mA for 50-90 minutes. Blocked the membrane with 5% non-fat milk/TBS for 1.5 hour at RT. The membrane was incubated with rabbit anti-HMGB1 antigen affinity purified polyclonal antibody (Catalog # A00066-1) at 0.5 ug/mL overnight at 4°C, then washed with TBS-0.1%Tween 3 times with 5 minutes each and probed with a goat anti-rabbit IgG-HRP secondary antibody at a dilution of 1:5000 for 1.5 hour at RT. The signal is developed using an Enhanced Chemiluminescent detection (ECL) kit (Catalog # EK1002) with Tanon 5200 system. A specific band was detected for HMGB1 at approximately 25 kDa. The expected band size for HMGB1 is at 25 kDa.

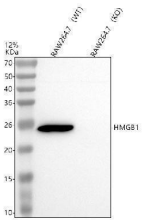

Western blot analysis of HMGB1 using anti-HMGB1 antibody (A00066-1). Electrophoresis was performed on a 12% SDS-PAGE gel at 80V (Stacking gel) / 120V (Resolving gel) for 2 hours. The sample well of each lane was loaded with 30 ug of sample under reducing conditions. Lane 1: mouse RAW264.7- WT whole cell lysates, Lane 2: mouse RAW264.7-Hmgb1 KO whole cell lysates. After electrophoresis, proteins were transferred to a nitrocellulose membrane at 150 mA for 50-90 minutes. Blocked the membrane with 5% non-fat milk/TBS for 1.5 hour at RT. Then the membrane was incubated with rabbit anti-HMGB1 antigen affinity purified polyclonal antibody (A00066-1) at 0.5 ug/mL overnight at 4°C, then washed with TBS-0.1%Tween 3 times with 5 minutes each and probed with a goat anti-rabbit IgG-HRP secondary antibody (Catalog # BA1054) at a dilution of 1:5000 for 1.5 hour at RT. The signal is developed using an ECL Plus Western Blotting Substrate (Catalog # AR1196-200) with Tanon 5200 system. A specific band was detected for HMGB1 at approximately 25 kDa. The expected band size for HMGB1 is at 25 kDa.

IHC analysis of HMGB1 using anti-HMGB1 antibody (A00066-1). HMGB1 was detected in paraffin-embedded section of mouse liver tissues. Heat mediated antigen retrieval was performed in citrate buffer (pH6, epitope retrieval solution) for 20 mins. The tissue section was blocked with 10% goat serum. The tissue section was then incubated with 1ug/ml rabbit anti-HMGB1 Antibody (A00066-1) overnight at 4°C. Biotinylated goat anti-rabbit IgG was used as secondary antibody and incubated for 30

BOSTER BIOLOGICAL TECHNOLOGY
3942 B Valley Ave, Pleasanton, CA 94566
888-466-3604 | support@bosterbio.com | www.bosterbio.com

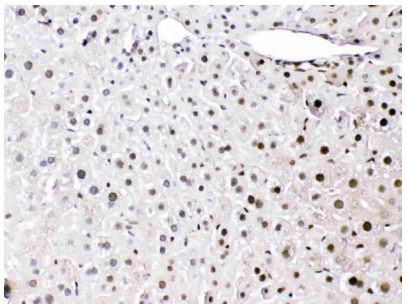

minutes at 37°C. The tissue section was developed using Strepavidin-Biotin-Complex (SABC)(Catalog # SA1022) with DAB as the chromogen.

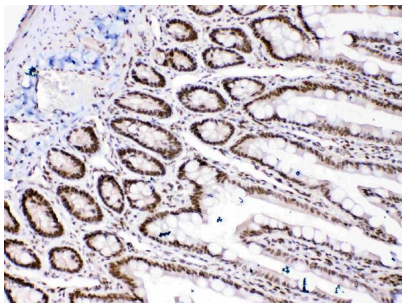

IHC analysis of HMGB1 using anti-HMGB1 antibody (A00066-1). HMGB1 was detected in paraffin-embedded section of rat intestine tissues. Heat mediated antigen retrieval was performed in citrate buffer (pH6, epitope retrieval solution) for 20 mins. The tissue section was blocked with 10% goat serum. The tissue section was then incubated with 1ug/ml rabbit anti-HMGB1 Antibody (A00066-1) overnight at 4°C. Biotinylated goat anti-rabbit IgG was used as secondary antibody and incubated for 30 minutes at 37°C. The tissue section was developed using Strepavidin-Biotin-Complex (SABC)(Catalog # SA1022) with DAB as the chromogen.

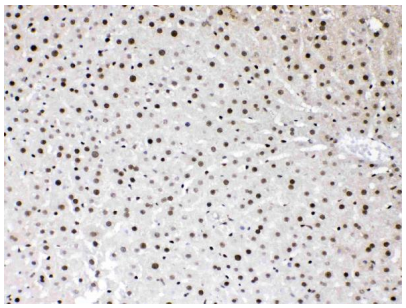

IHC analysis of HMGB1 using anti-HMGB1 antibody (A00066-1). HMGB1 was detected in paraffin-embedded section of rat liver tissues. Heat mediated antigen retrieval was performed in citrate buffer (pH6, epitope retrieval solution) for 20 mins. The tissue section was blocked with 10% goat serum. The tissue section was then incubated with 1ug/ml rabbit anti-HMGB1 Antibody (A00066-1) overnight at 4°C. Biotinylated goat anti-rabbit IgG was used as secondary antibody and incubated for 30 minutes at 37°C. The tissue section was developed using Strepavidin-Biotin-Complex (SABC)(Catalog # SA1022) with DAB as the chromogen.

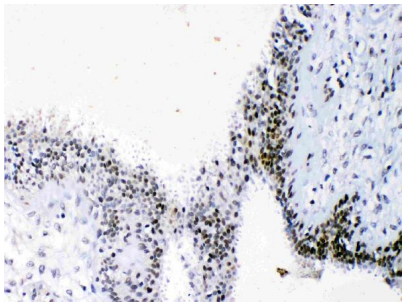

IHC analysis of HMGB1 using anti-HMGB1 antibody (A00066-1). HMGB1 was detected in paraffin-embedded section of human mammary cancer tissues. Heat mediated antigen retrieval was performed in citrate buffer (pH6, epitope retrieval solution) for 20 mins. The tissue section was blocked with 10% goat serum. The tissue section was then incubated with 1ug/ml rabbit anti-HMGB1 Antibody (A00066-1) overnight at 4°C. Biotinylated goat anti-rabbit IgG was used as secondary antibody and incubated for 30 minutes at 37°C. The tissue section was developed using Strepavidin-Biotin-Complex (SABC)(Catalog # SA1022) with DAB as the chromogen.

IHC analysis of HMGB1 using anti-HMGB1 antibody (A00066-1). HMGB1 was detected in paraffin-embedded section of human placenta tissues. Heat mediated antigen retrieval was performed in citrate buffer (pH6, epitope retrieval solution) for 20 mins. The tissue section was blocked with 10% goat serum. The tissue section was then

BOSTER BIOLOGICAL TECHNOLOGY
3942 B Valley Ave, Pleasanton, CA 94566
888-466-3604 | support@bosterbio.com | www.bosterbio.com

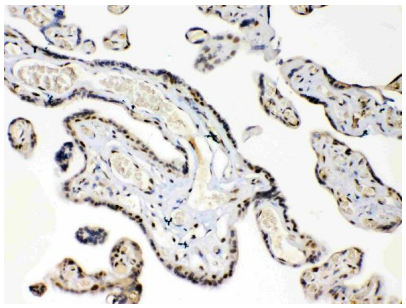

incubated with 1ug/ml rabbit anti-HMGB1 Antibody (A00066-1) overnight at 4°C. Biotinylated goat anti-rabbit IgG was used as secondary antibody and incubated for 30 minutes at 37°C. The tissue section was developed using Strepavidin-Biotin-Complex (SABC)(Catalog # SA1022) with DAB as the chromogen.

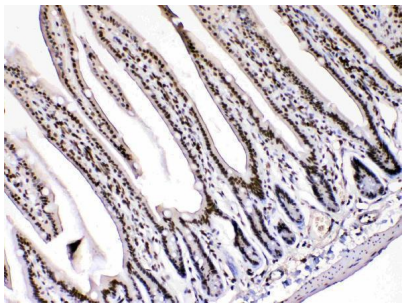

IHC analysis of HMGB1 using anti-HMGB1 antibody (A00066-1). HMGB1 was detected in paraffin-embedded section of mouse intestine tissues. Heat mediated antigen retrieval was performed in citrate buffer (pH6, epitope retrieval solution) for 20 mins. The tissue section was blocked with 10% goat serum. The tissue section was then incubated with 1ug/ml rabbit anti-HMGB1 Antibody (A00066-1) overnight at 4°C. Biotinylated goat anti-rabbit IgG was used as secondary antibody and incubated for 30 minutes at 37°C. The tissue section was developed using Strepavidin-Biotin-Complex (SABC)(Catalog # SA1022) with DAB as the chromogen.

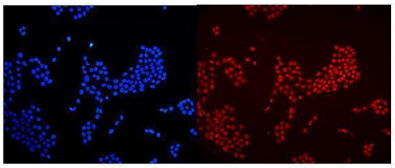

IF analysis of HMGB1 using anti-HMGB1 antibody (A00066-1). HMGB1 was detected in immunocytochemical section of A431 cells. Enzyme antigen retrieval was performed using IHC enzyme antigen retrieval reagent (AR0022) for 15 mins. The cells were blocked with 10% goat serum. And then incubated with 2ug/mL rabbit anti-HMGB1 Antibody (A00066-1) overnight at 4°C. DyLight®594 Conjugated Goat Anti-Rabbit IgG (BA1142) was used as secondary antibody at 1:100 dilution and incubated for 30 minutes at 37°C. The section was counterstained with DAPI. Visualize using a fluorescence microscope and filter sets appropriate for the label used.

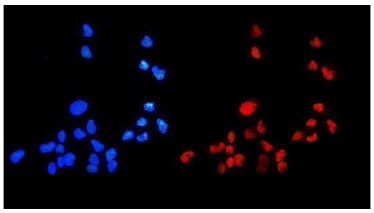

IF analysis of HMGB1 using anti- HMGB1 antibody (A00066-1). HMGB1 was detected in immunocytochemical section of U20S cells. Enzyme antigen retrieval was performed using IHC enzyme antigen retrieval reagent (AR0022) for 15 mins. The cells were blocked with 10% goat serum. And then incubated with 2ug/mL rabbit anti- HMGB1 Antibody (A00066-1) overnight at 4°C. DyLight®594 Conjugated Goat Anti-Rabbit IgG (BA1142) was used as secondary antibody at 1:100 dilution and incubated for 30 minutes at 37°C. The section was counterstained with DAPI. Visualize using a fluorescence microscope and filter sets appropriate for the label used.

IF analysis of HMGB1 using anti-HMGB1 antibody (A00066-1). HMGB1 was detected in an immunocytochemical section of Mouse 4T1 cells. Enzyme antigen retrieval was performed using IHC enzyme antigen retrieval reagent (AR0022) for 15 mins. The cells were

BOSTER BIOLOGICAL TECHNOLOGY
3942 B Valley Ave, Pleasanton, CA 94566
888-466-3604 | support@bosterbio.com | www.bosterbio.com

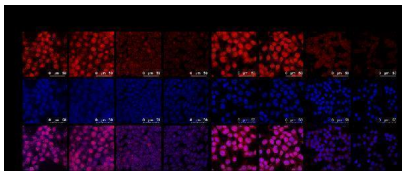

blocked with 10% goat serum. And then incubated with 5 ug/mL rabbit anti-HMGB1 Antibody (A00066-1) overnight at 4°C. DyLight 550-conjugated Goat Anti-Mouse was used as secondary antibody incubated for 30 minutes at 37°C. The section was counterstained with DAPI. Visualize using a laser confocal microscope with filter sets appropriate for the label used.

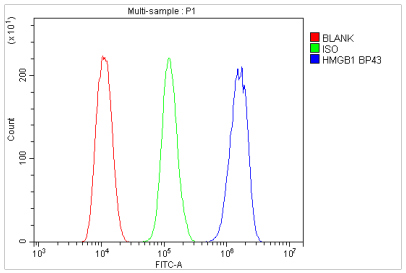

Flow Cytometry analysis of THP-1 cells using anti-HMGB1 antibody (A00066-1). Overlay histogram showing THP-1 cells stained with A00066-1 (Blue line).To facilitate intracellular staining, cells were fixed with 4% paraformaldehyde and permeabilized with permeabilization buffer. The cells were blocked with 10% normal goat serum. And then incubated with rabbit anti-HMGB1 Antibody (A00066-1, 1ug/1x106 cells) for 30 min at 20°C. DyLight®488 conjugated goat anti-rabbit IgG (BA1127, 5-10ug/1x106 cells) was used as secondary antibody for 30 minutes at 20°C. Isotype control antibody (Green line) was rabbit IgG (1ug/1x106) used under the same conditions. Unlabelled sample without incubation with primary antibody and secondary antibody (Red line) was used as a blank control.

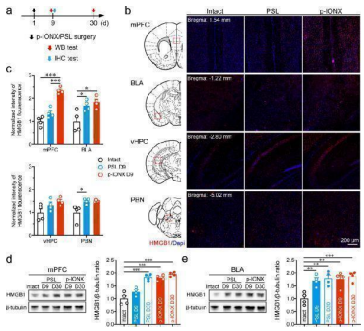

HMGB1 expression in the mPFC was increased temporally in parallel to comorbid anxiety in neuropathic pain. a Schedule of experimental procedures. b Representative photomicrographs of HMGB1 immunostaining in the mPFC, BLA, vHPC and PBN. Scale bar, 200 um. c Quantification of HMGB1 fluorescence intensity in the mPFC, BLA, vHPC and PBN on D9 PO. d, e Representative images of protein bands in western blotting (left) and quantification of HMGB1 expression (right) in the mPFC (d) and BLA (e) on D9 and D30 PO. *, ** and *** indicate P

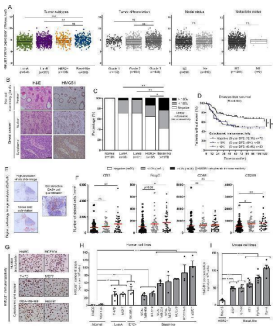

HMGB1 is highly secreted by basal-like breast cancer cells and its tumor-specific cytoplasmic expression is associated with immune tolerance and poor outcome. (A) The METABRIC dataset was used for analyzing HMGB1 expression level in breast cancers according to molecular subtypes, histologic grades, nodal and metastatic statuses. (B) Representative pictures of normal mammary glands and breast cancers stained for HMGB1. Note the two distinct HMGB1 staining patterns detected in tumor specimens: nuclear versus cytoplasmic. (C) Semiquantitative evaluation of cytoplasmic HMGB1 immunoreactivity (negative, 0%–10% or >10% positive cells) in both normal mammary glands (n=120) and neoplasms (LumA, n=35; LumB, n=31; HER2+, n=37; basal-like, n=172). (D) Disease-free survival of patients treated for basal-like breast cancer according to cytoplasmic HMGB1 expression (negative, n=72; 0%–10%, n=61; >10%, n=39). This latter parameter was clearly found to be an independent prognostic factor. (E) Illustration of the different steps for DAB-positive cell quantification using computerized image analysis (QuPath). (F) CD3 + , Foxp3 + , CD68 + and CD206 + cell infiltrations in microenvironment of basal-like breast tumors. Whereas the global number (CD68 +) did not significantly change, an increased density

of CD206 + M2 macrophages was detected in cytoplasmic HMGB1-positive cancers. A similar increase was also reported with Foxp3 + Treg lymphocytes. the number of positive cells was reported to tumor area (mm 2). (G) Representative examples of normal (HMEC and MCF10A) and malignant cells (LumA: T-47D and MCF7; basal-like: MDA-MB-468 and Hs578T) stained for HMGB1. Note the exclusive nuclear immunoreactivity displayed by normal mammary cells. Secretion/release of HMGB1 analyzed by ELISA in (H) human and (I) mouse cell culture supernatants. High concentrations were especially detected in cell cultures derived from triple negative/basal-like tumors. The means±SEM (plus each individual data point) for at least three independent experiments are represented. The scale bar represents 100 µm. Asterisks indicate statistically significant differences (*p

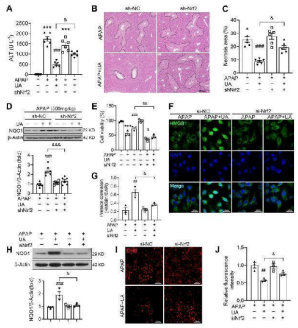

UA alleviates APAP-induced oxidative stress through Nrf2 signaling pathway. The mice were pretreated with AAV8-sh-Nrf2 (5 × 10 10 vg/mL) or Scramble shRNA via tail vein injection. One week after AAV infection, the mice were challenged with APAP injection with or without UA treatment (50 mg/kg). The liver tissue and serum were harvested at 12 h after APAP challenge. n = 6 mice per group. (A) Serum ALT levels from different groups. (B) Representative images of hematoxylin and eosin-stained liver sections, scale bar: 100 um. (C) The quantification of necrosis area of the liver tissue. (D) Representative immunoblots and analysis of NQO1 expression in mice were treated with or without Nrf2 shRNA. (E) The L02 cells were transfected with the siNrf2 RNA or Scramble siRNA for 48 h and then treated with or without UA (5 uM) in the presence or absence of APAP (10 mM) for 24 h. Cell viability was determined by CCK8 assay. (F) HMGB1 immunofluorescence of L02 cells. scale bar: 50 um. (G) Quantification of colocalization of HMGB1 and nuclei. (H) Representative immunoblots and analysis of NQO1 expression in L02 cells. (I) Representative images of DHE staining of L02 cells, scale bar, 100 um. (J) The quantification of the DHE positive intensity. Data are expressed as mean ± SEM. The in vitro experiment was repeated at least 3 times. *** P < 0.001 vs. CTL; ## P < 0.01, ### P < 0.001 vs. APAP; & P < 0.05, &&& P < 0.001 vs. siNC-APAP + UA or sh-NC-APAP + UA.Index in PubMed under a CC BY license. PMID: 35342347

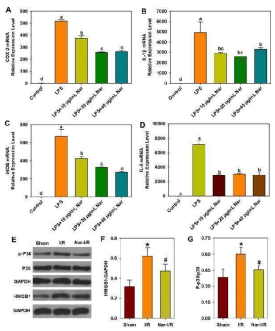

Anti-inflammation of naringin in vitro and in vivo. A – D Effect of naringin on LPS-induced mRNA expression of COX-2, iNOS, IL-1beta, and IL-6 in RAW 264.7 macrophages. The concentration of LPS is 1 ug/mL. A COX-2 mRNA relative expression level; B IL-1beta mRNA relative expression level; C iNOS mRNA relative expression level; D IL-6 mRNA relative expression level. Different letters show significant differences (p

UA Protected against Acetaminophen-induced Cytotoxicity in

BOSTER BIOLOGICAL TECHNOLOGY
3942 B Valley Ave, Pleasanton, CA 94566
888-466-3604 | support@bosterbio.com | www.bosterbio.com

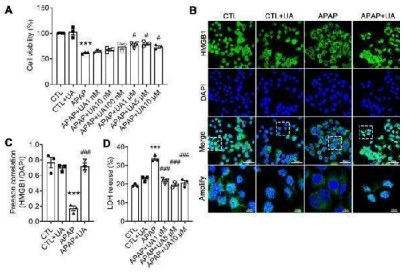

vitro . (A) L02 hepatocytes were subjected to UA at different concentrations with or without APAP (10 mM) for 24 h. Cell viability was determined by CCK8 assay. (B) HMGB1 (green) staining of L02 cells. Representative images with amplification indicating example cells with cytoplasmic HMGB1 staining and hollow nuclei (scale bars: 50 um for upper and 10 um for bottom), and quantification of colocalization of HMGB1 and nuclei by Image J software in at least 20 randomly selected individual cells. (C) Quantification of LDH released into the culture medium of L02 cells. Data were represented as the means ± SEM, the experiment was repeated at least 3 times, *** P < 0.001 vs. CTL; # P < 0.05, ### P < 0.001 vs. APAP.Index in PubMed under a CC BY license. PMID: 35342347

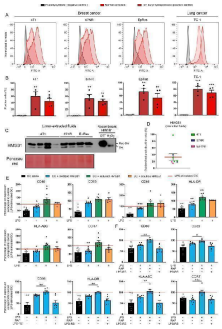

A significant fraction of HMGB1 contained in tumor-extruded fluids is in its oxidized form and displays RAGE-dependent tolerogenic properties. (A, B) The ROS accumulation in both breast (4T1, 67NR, EpRas) and lung (TC-1) cancer cells used in the present study was assessed by flow cytometry. N-acetylcysteine (5 mM) and tert-butyl hydroperoxide (100 µM) were used as negative and positive controls, respectively. Results represent the means±SEM of four independent experiments (each individual data point is shown). (C) The redox state of extracellular HMGB1 contained in tumor-extruded fluids was analyzed by Western blot. All samples were directly alkylated in order to ‘freeze’ the redox state of HMGB1 molecules. Recombinant HMGB1 (0.5 µg) incubated with either H 2 O 2 or DTT (and then alkylated) were used as controls. (D) Oxidized/reduced-disulfide HMGB1 ratio (%) was calculated from the Western blot bands using ImageJ software. (E) DCs were incubated with terminally oxidized, fully reduced or disulfide HMGB1 for 24 hours before being stimulated with LPS for 24 hours. The expression of cell-surface molecules (CD80, CD83, CD86, HLA-DR, HLA-ABC and CCR7) was then measured by flow cytometry. All data were normalized to LPS-stimulated DC. Data represent the relative mean fluorescent intensity (MFI)±SEM of at least five independent experiments (each individual data point is shown). (F) DCs were incubated with terminally oxidized HMGB1 for 24 hours before being stimulated with LPS for 24 hours. When indicated, an inhibitor of RAGE (10 µM RAP) or TLR4 (2 µM LPS-RS) was added in the cell culture. The expression of DC activation markers was determined by flow cytometry. All data were normalized to LPS-stimulated DC. The relative MFI±SEM of 7 independent experiments are shown. Asterisks indicate statistically significant differences (*p

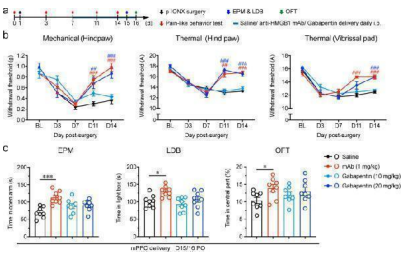

Systemic anti-HMGB1 mAb simultaneously alleviated pain sensitization and anxiety after p-IONX. a Schedule of experimental procedures. b Paw withdrawal thresholds to mechanical stimulation and noxious heat stimulation at the left hind paw and head withdrawal threshold to noxious heat stimulation at the left vibrissal pad before and after p-IONX. ## and ### indicate P

BOSTER BIOLOGICAL TECHNOLOGY
3942 B Valley Ave, Pleasanton, CA 94566
888-466-3604 | support@bosterbio.com | www.bosterbio.com

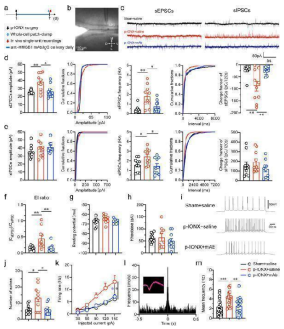

Systemic anti-HMGB1 mAb reversed the hyperexcitability of pyramidal neurons in mPFC layer 2/3 after p-IONX. a Schedule of experimental procedures. Anti-HMGB1 mAb was administered intraperitoneally. b Example image of whole cell patch-clamp recordings on mPFC layer 2/3 pyramidal neurons. Scale bar, 150 um. c Example traces of sEPSCs and sIPSCs in sham + saline, p-IONX + saline and p-IONX + anti-HMGB1 mAb groups. d, e Amplitude, frequency and charge transfer of sEPSCs (d) and sIPSCs (e). f Quantification of E/I ratio (| CsEPSC | /CsIPSC). g, h Resting potential (g) and rheobase (the lowest current that evoked action potential firing, h). i, j Representative traces of firing (i) and number of spikes (j) of action potentials evoked by injecting current at two-fold of rheobase. k Firing rate of action potentials evoked by step-current injection. l Autocorrelation and waveform (inset) of a representative glutamatergic neuron in in vivo single-unit recordings. m Mean frequency of spontaneous firing. *, ** and *** indicate P

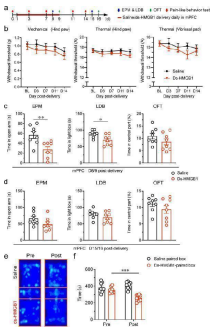

HMGB1 in the mPFC was sufficient to induce anxiety-like behaviors and aversion but not pain sensitization in naïve mice. a Schedule of experimental procedures. b Paw withdrawal thresholds to mechanical stimulation and noxious heat stimulation at the left hind paw and head withdrawal threshold to noxious heat stimulation at the left vibrissal pad. c, d Anxiety-like behaviors measured by EPM, LDB and OFT on D8/9 (c) and D15/16 (d) after administration. e Representative heat maps in the CPP test. f Time spend by mice in the saline- and ds-HMGB1-paired boxes. *, ** and *** indicate P

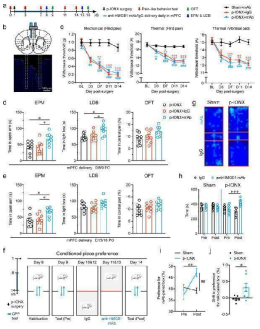

Local neutralization of HMGB1 in the mPFC reduced anxiety-like behaviors and aversion but not pain sensitization after p-IONX. a Schedule of procedures of mPFC drug delivery experiments in the early phase after p-IONX. b Schematic (upper) and representative photomicrograph (lower) of the cannula implantation in bilateral mPFC for local infusion of agents. Dashed lines indicate the trace of implanted canula. Scale bar, 100 um. c Paw withdrawal thresholds to mechanical stimulation and noxious heat stimulation at the left hind paw and head withdrawal threshold to noxious heat stimulation at the left vibrissal pad before and after p-IONX. *, ** and *** indicate P

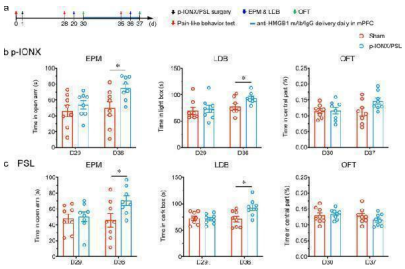

HMGB1 upregulation in the mPFC maintained comorbid anxiety in neuropathic pain. a Schedule of procedures of mPFC drug delivery experiments in the late phase after p-IONX. b , c Anxiety-like behaviors measured by EPM, LDB and OFT on D29/30 and D36/37 after p-IONX and PSL, respectively. * indicates P

Cellular and subcellular distribution of HMGB1 in the mPFC after p-IONX in MRL/MPJ mice . a-c Representative

BOSTER BIOLOGICAL TECHNOLOGY
3942 B Valley Ave, Pleasanton, CA 94566
888-466-3604 | support@bosterbio.com | www.bosterbio.com

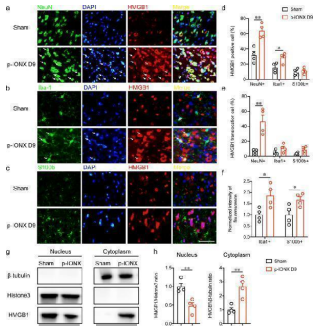

photomicrographs indicating the cellular distribution of HMGB1 in neurons (NeuN + , a), microglia (Iba1 + , b) and astrocytes (S100b + , c) in the mPFC on D9 PO. DAPI was used to label nuclei. Scale bar, 50 um. d Percentage of HMGB1-positive cells in neurons (NeuN +), microglia (Iba1 +) and astrocytes (S100b +) on D9 PO in the mPFC. e Percentage of cells with HMGB1 cytoplasmic translocation in neurons (NeuN +), astrocytes (S100b +) and microglia (Iba1 +) on D9 PO in the mPFC. f Quantification of Iba1 and S100b fluorescence intensity in the mPFC. g-h Representative images of western blot bands (g) and quantification of HMGB1 (h) in nuclear and cytoplasmic fractions from the mPFC on D9 PO. * and ** indicate P

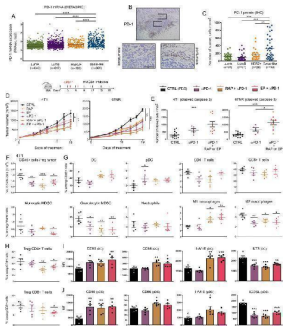

Extracellular HMGB1 blockade enhances anti-PD-1-induced inhibition of tumor growth in vivo. (A) PD-1 mRNA expression (PDCD1 gene) in the four major molecular subtypes of breast cancer was determined using the METABRIC public dataset. (B) Representative example of breast cancer stained for PD-1. Positive cells were observed in the epithelial component of the tumor as well as in the stroma surrounding cancer cells. (C) PD-1 + cell infiltration within tumor microenvironment was determined by computerized counting. Each point represents the number of positive cells/mm 2 for one independent tumor specimen. (D) Mouse breast cancer cells (4T1 and 67NR) were orthotopically injected into the mammary fat pad of immunocompetent BALB/c mice. Anti-PD-1 antibody was tested alone (i.p. injection of 200 µg at days 4, 7 and 11) and in combination with HMGB1 inhibitors (RAP (10 µM/kg) and EP (1 mM/kg), treatment at 3 day intervals). In parallel, the anticancer efficacy of these combination regimens was also compared with that displayed by each individual HMGB1 inhibitor used in monotherapy. The mean tumor volumes±SEM are represented. (E) The apoptotic cancer cells (cleaved caspase 3 +) were detected by immunohistochemistry and quantified using QuPath software. The number of positive cells was reported to tumor area (mm 2). (F) The total number of (CD45 +) immune cells per milligram of tumor was determined in the different treatment groups. (G) Scatter dot plots illustrating the percentage of each individual immune cell population (DC, PDC, CD4 + and CD8 + T cells, monocytic and granulocytic MDSC, neutrophils, M1 and M2 macrophages) among CD45 + cells in both control and treated groups. Reduced densities of granulocytic MDSC as well as an increase of M1 macrophages were especially observed in case of combination therapy. The intratumoral immune cells were analyzed in five mice per condition. (H) Scatter dot plots showing the percentage of tumor-infiltrating Treg (Foxp3 +) CD4 + and CD8 + cells among total CD4 + and CD8 + populations in the different treatment groups. the activation status of DC (I) and pDC (J) was determined by flow cytometry. the expression of several surface markers (CD80, CD86, I-A/I-E, ILT3 and ICOSL) was analyzed. Data represent the mean fluorescent intensity (MFI)±SEM of 5 independent experiments in each group (each individual data point is shown). The scale bar represents 100 µm. Asterisks indicate statistically significant differences (*p

BOSTER BIOLOGICAL TECHNOLOGY
3942 B Valley Ave, Pleasanton, CA 94566
888-466-3604 | support@bosterbio.com | www.bosterbio.com

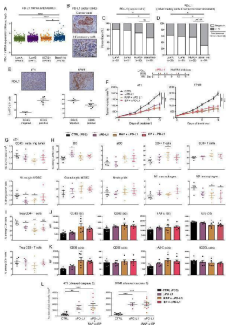

Combination of anti-PD-L1 with HMGB1 inhibitors strongly inhibits tumor growth in syngeneic mouse models of basal-like breast cancer. (A) mRNA level of PD-L1 (CD274 gene) in the four major molecular subtypes of breast cancer was determined using the METABRIC public dataset. (B) Representative example of breast cancer stained for PD-L1. Positive signals were detected on cancer cells and/or on inflammatory cells within tumor microenvironment. Semiquantitative evaluation of PD-L1 immunoreactivity (negative or >1% membrane staining) displayed by cancer cells (C) or inflammatory cells infiltrating the tumor microenvironment (D). The analyzed cancer specimens were categorized into the four molecular subtypes of breast cancer (LumA, LumB, HER2 + and basal-like). (E) The percentage of PD-L1 + cells in both epithelial/cancer (CD45 -) and inflammatory (CD45 +) components of untreated harvested 4T1/67NR tumors was determined by flow cytometry. Note the distinct profile displayed by these two cell lines. (F) Mouse breast cancer cells (4T1 and 67NR) were orthotopically injected into the mammary fat pad of immunocompetent BALB/c mice. Anti-PD-L1 antibody was tested alone (i.p. injection of 100 µg at days 4, 7 and 11) and in combination with HMGB1 inhibitors (RAP (10 µM/kg) and EP (1 mM/kg), treatment at 3-day intervals). The mean tumor volumes±SEM are represented. (G) The total number of (CD45 +) immune cells per milligram of tumor was determined in the different treatment groups by flow cytometry. (H) Scatter dot plots illustrating the percentage of each individual immune cell population (DC, PDC, CD4 + and CD8 + T cells, monocytic and granulocytic MDSC, neutrophils, M1 and M2 macrophages) among CD45 + cells in both control and treated groups. The intratumoral immune cell infiltration was analyzed in five mice per condition. (I) scatter dot plots showing the percentage of tumor-infiltrating Treg (Foxp3 +) CD4 + and CD8 + cells among total CD4 + and CD8 + populations in the different treatment groups. The activation status of DC (J) and pDC (K) was determined by flow cytometry. the expression of several surface markers (CD80, CD86, I-A/I-E, ILT3 and ICOSL) was assessed. Data represent the mean fluorescent intensity (MFI)±SEM of five independent experiments in each group (each individual data point is shown). (L) The apoptotic cancer cells (cleaved caspase 3 +) were detected by immunohistochemistry and quantified using QuPath software. The number of positive cells was reported to tumor area (mm 2). The scale bar represents 100 µm. Asterisks indicate statistically significant differences (*p

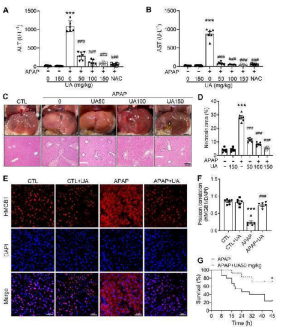

UA Protected against Acetaminophen-induced liver injury in vivo . (A) Serum ALT and (B) AST activities in mice with various concentrations of Urolithin A in the presence or absence of APAP administration (500 mg/kg), n = 6. (C) The representative image of liver tissue (scale bar: 500 mm) and representative image of H&E-stained liver sections at 100 × magnification, scale bar: 200 um. APAP-induced centrilobular necrosis was indicated by the dotted line. (D) The quantification of necrosis area of the liver tissue, n = 6. (E) HMGB1 staining of liver sections (scale bar: 50 um). (F)

BOSTER BIOLOGICAL TECHNOLOGY
3942 B Valley Ave, Pleasanton, CA 94566
888-466-3604 | support@bosterbio.com | www.bosterbio.com

Quantification of colocalization of HMGB1 and nuclei by Image J (NIH, Bethesda, MD) software, n = 6. (G) The survival rate in the APAP challenged (750 mg/kg) mice with or without UA treatment (15 mice per group). Data were represented as the means ± SEM. *** P < 0.001 vs. CTL; # P < 0.05, ### P < 0.001 vs. APAP.Index in PubMed under a CC BY license. PMID: 35342347

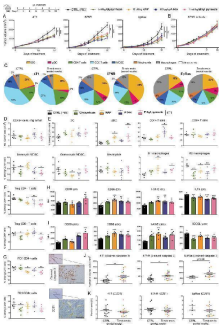

Extracellular HMGB1 blockade inhibits the growth of pre-established solid tumors in immunocompetent mice through activating anticancer immune responses. (A) Mouse basal-like breast cancer cells (4T1, 67NR and EpRas) were orthotopically injected into the mammary fat pad of immunocompetent BALB/c mice. Tumor-bearing mice were then treated at 3-day intervals with PBS (control) or HMGB1 inhibitors (glycyrrhizin (1 nM/kg), RAP (10 μM/kg), a box (500 μg/kg) and EP (1 mM/kg)). The mean tumor volumes±SEM are represented. (B) HMGB1 inhibitors were tested in nude mice implanted with 67NR cells. Note the absence of beneficial effect in these latter immunocompromised mice, indicating the dependence on the adaptive immune responses. (C) At day 17, 19 or 20 (depending on the analyzed cell line), tumors were harvested, CD45 + immune cells were isolated and analyzed by flow cytometry. The proportions of each analyzed immune cell population in both control and treated groups (pooled results) are shown. Note the drastic reduction of MDSC following extracellular HMGB1 blockade. (D) Total number of (CD45 +) immune cells per milligram of tumor in both control and treated groups. (E) Scatter dot plots showing the percentage of each individual immune cell population (DC, PDC, CD4 + and CD8 + T cells, monocytic and granulocytic MDSC, neutrophils, M1 and M2 macrophages) among CD45 + cells in the different treatment groups. an increased M1/M2 ratio of macrophages was observed in most HMGB1 inhibitor-treated tumors. The intratumoral immune cells were analyzed in five mice per condition. (F) Scatter dot plots illustrating the percentage of tumor-infiltrating Treg (Foxp3 +) CD4 + and CD8 + cells among total CD4 + and CD8 + populations in the different treatment groups. (G) Scatter dot plots illustrating the percentage of tumor-infiltrating PD-1 + CD4 + and PD-1 + CD8 + cells among total CD4 + and CD8 + populations in the treatment groups. The activation status of both DC (H) and PDC (I) in the different treatment groups was also determined by analyzing the expression of several cell surface markers (CD80, CD86, I-A/I-E, ILT3 and ICOSL). Data represent the mean fluorescent intensity (MFI)±SEM of 5 independent experiments in each group (each individual data point is shown). The number of apoptotic cancer cells (cleaved caspase 3 +) (J) as well as the density of blood vessels within tumor microenvironment (CD31 +) (K) were determined by computerized counting (using QuPath software). The number of cleaved caspase 3 + cells and the percentage of CD31 + pixels were reported to tumor area. The scale bar represents 100 μm. Asterisks indicate statistically significant differences (*p

11 Publications Citing This Product

BOSTER BIOLOGICAL TECHNOLOGY
3942 B Valley Ave, Pleasanton, CA 94566
888-466-3604 | support@bosterbio.com | www.bosterbio.com

1. PubMed ID: 10.5812/hepatmon.23552, Association of Upregulated HMGB1 and c-IAP2 Proteins With Hepatocellular Carcinoma Development and Progression

2. PubMed ID: 10.1136/jitc-2020-001966, Extracellular HMGB1 blockade inhibits tumor growth through profoundly remodeling immune microenvironment and enhances checkpoint inhibitor-based immunotherapy

3. PubMed ID: 10.1097/FJC.0000000000000353, Effects of Ethyl Pyruvate in Preventing the Development of Diet-induced Atherosclerosis by Blocking the HMGB1 Expression in ApoE-Deficient Mice

Visit bosterbio.com/anti-hmgb1-picoband-trade-antibody-a00066-1-boster.html to see all 11 publications.

Anti-HMGB1 Antibody

For Research Use Only. Not for use in diagnostic procedures.